Journal of Instrumentation

Experimental ion mobility measurements in Xe-C_2H_6

To cite this article: J.M.C. Perdigoto *et al* 2017 *JINST* **12** P10011

Published by IOP Publishing for Sissa Medialab

Received: *March 13, 2017*
Accepted: *September 26, 2017*
Published: *October 19, 2017*

Experimental ion mobility measurements in Xe-C_2H_6

J.M.C. Perdigoto,[a,b] **A.F.V. Cortez,**[a,b,1] **R. Veenhof,**[c,d] **P.N.B. Neves,**[e] **F.P. Santos,**[a,b] **F.I.G.M. Borges**[a,b] **and C.A.N. Conde**[a,b]

[a] *Laboratory of Instrumentation and Experimental Particle Physics – LIP, Rua Larga, 3004-516 Coimbra, Portugal*
[b] *Department of Physics, Faculty of Science and Technology, University of Coimbra, Rua Larga, 3004-516 Coimbra, Portugal*
[c] *Physics Department, CERN, Geneve 23, CH-1211 Switzerland*
[d] *Physics Department, Faculty of Arts and Sciences, Uludağ University, 16059 Bursa, Turkey*
[e] *Closer Consultoria, LDA, Av. Engenheiro Duarte Pacheco, Torre 2, 14o-C, Lisboa, 1070-102 Portugal*

E-mail: andre.f.cortez@gmail.com

Abstract: In this paper we present the results of the ion mobility measurements made in gaseous mixtures of xenon (Xe) with ethane (C_2H_6) for pressures ranging from 6 to 10 Torr (8–10.6 mbar) and for low reduced electric fields in the 10 Td to 25 Td range (2.4–6.1 kV·cm^{-1} · bar^{-1}), at room temperature. The time of arrival spectra revealed two peaks throughout the entire range studied which were attributed to ion species with 3-carbons ($C_3H_5^+$, $C_3H_6^+$ $C_3H_8^+$ and $C_3H_9^+$) and with 4-carbons ($C_4H_7^+$, $C_4H_9^+$ and $C_4H_{10}^+$). Besides these, and for Xe concentrations above 70%, a bump starts to appear at the right side of the main peak for reduced electric fields higher than 20 Td, which was attributed to the resonant charge transfer of $C_2H_6^+$ to C_2H_6 that affects the mobility of its ion products ($C_3H_8^+$ and $C_3H_9^+$). The time of arrival spectra for Xe concentrations of 20%, 50%, 70% and 90% are presented, together with the reduced mobilities as a function of the Xe concentration calculated from the peaks observed for the low reduced electric fields and pressures studied.

Keywords: Charge transport and multiplication in gas; Ionization and excitation processes; Gaseous detectors; Ion sources (positive ions, negative ions, electron cyclotron resonance (ECR), electron beam (EBIS))

[1] Corresponding author.

https://doi.org/10.1088/1748-0221/12/10/P10011

2017 JINST 12 P10011

Contents

2017 JINST 12 P10011

1 Introduction

Measuring the mobility of ions in gases is relevant in several areas, from physics to chemistry, e.g. in gaseous radiation detectors modelling and in the understanding of the pulse shape formation [1–3], and also in IMS (Ion Mobility Spectrometry) a technique used for the detection of narcotics and explosives [4]. One of these examples are the so-called Transition Radiation Detectors (TRDs), used for particle identification at high momenta [5, 6]. Xenon (Xe) is considered to be the best choice for the main gas, while the choice of the quencher is determined by different parameters [3]. For instance, methane, CH_4, is an effective quencher but due to its flammability its usage is limited [3]. Nowadays CO_2 is widely used although experiments such as the H1 experiment in HERA Collaboration still make use of Xe-C_2H_6 based mixtures with Helium (He) [6]. In order to fully understand and model these detectors it is important to have detailed information on the transport properties of ions.

Using the experimental method described in detail in [7], the mobility of ions in xenon-ethane (Xe-C_2H_6) gas mixtures is measured at pressures in the 6 to 8 Torr (8 to 10.6 mbar) range and for reduced electric fields commonly used in gaseous detectors, extending previous studies developed in our group for other gases [7–17].

1.1 Ion mobility

When we consider a group of ions moving in a weakly ionized gas under the influence of low uniform electric field, these ions will collide with neutral gas molecules, losing energy in collisions while gaining energy from the electric field, eventually reaching a steady state. The resulting

average velocity of the group of ions, v_d, also known as drift velocity, is proportional to the electric field, E, and so:

$$v_d = KE \tag{1.1}$$

where K is the mobility of the ions and E is the intensity of the drift electric field. This relation is applicable for low E/N, i.e., when the energy gained from the field between collisions is below the thermal energy [4, 18]. K is usually expressed in terms of reduced mobility K_0, suppressing the dependence of the mobility values on the gas pressure. Thus

$$K_0 = KN/N_0 \tag{1.2}$$

where N is the gas number density and N_0 is the Loschmidt number ($N_0 = 2.68678 \times 10^{19}\,\mathrm{cm}^{-3}$ for 273.15 K and 101.325 kPa according to NIST [19]). The mobility measurements are usually presented as a function of the reduced electric field E/N in units of Td (1 Td = $10^{-21}\,\mathrm{V{\cdot}m^2}$). The reduced mobility obtained is expressed in terms of $\mathrm{cm^2 \cdot V^{-1} \cdot s^{-1}}$.

1.2 Langevin's theory

According to the Langevin's theory [20], one limiting value of the mobility is reached when the repulsion becomes negligible compared to the polarization effect. This limit is given by:

$$K_{\mathrm{pol}} = 13.88 \left(\frac{1}{\alpha\mu}\right)^{\frac{1}{2}} \tag{1.3}$$

where α is the neutral polarisability in cubic angstroms ($\alpha = 4.044 \pm 0.013\,\text{Å}^3$ for Xe [21] and $\alpha = 4.47 \pm 0.01\,\text{Å}^3$ for C_2H_6 [22]) and μ is the ion-neutral reduced mass in unified atomic mass units. Restrictions to the application of this theory may arise namely if resonant charge transfer occurs [18].

1.3 Blanc's law

Blanc's empirical law, which resulted from Blanc's work in the mobility of ions in binary gaseous mixtures, has proven to be most useful when determining ions' mobility using mixtures of gases. Blanc found that the mobility of ions in gaseous mixtures, obeyed a simple relationship as long as the charge transfer interaction is negligible compared to the polarization attraction and short-range repulsion between ion and atoms/molecules.

This relationship can be expressed as follows:

$$\frac{1}{K_{\mathrm{mix}}} = \frac{f_1}{K_{g1}} + \frac{f_2}{K_{g2}} \tag{1.4}$$

where K_{mix} is the reduced mobility of the ion in the binary mixture; K_{g1} and K_{g2} the reduced mobility of that same ion in an atmosphere of 100% of gas #1 and #2 respectively; f_1 and f_2 are the molar fraction of each gas in the binary mixture [23].

2017 JINST 12 P10011

2 Method and experimental setup

The mobility measurements presented in this study were obtained using the experimental system described in [7]. A UV flash lamp with a frequency of 10 Hz emits photons that impinge on a 250 nm thick CsI film deposited on the top of a Gas Electron Multiplier (GEM) placed inside a gas vessel. The photoelectrons released from the CsI film are guided through the GEM holes by the electric field created by applying an adequate voltage across its electrodes. After gaining enough energy, the electrons will ionize the gas molecules encountered along their paths. While the electrons are collected at the bottom of the GEM electrode, the cations formed will drift across a uniform electric field region towards a double grid; the first one acts as Frisch grid while the second one, at ground voltage, collects the ions' charge. The pulse collected at the collecting grid is converted from current to voltage by a pre-amplifier originating a time of arrival spectrum that is recorded in a digital oscilloscope (Tektronix TDS 1012), set to continuously average 128 pulses, and fed to a PC for further processing. After subtracting the background spectra, obtained without the voltage applied to the GEM (i.e. without drifting ions), to these time of arrival spectra, Gaussian curves are fitted to the peaks in the spectra using Matlab. The trigger in the system is set by the UV flash lamp, providing the initial time information.

Since the peaks' centroid corresponds to the average drift time of the ions along a known distance (4.2725 cm), the drift velocity is determined, and the mobility can then be calculated using expression 1.1. The system relies on the voltage across the GEM (V_{GEM}) to control the maximum energy of the electrons, which helps in the primary ion identification. Identifying the primary ions will allow to pinpoint secondary reaction paths that lead to the identification of the detected ions.

Since impurities play an important role in the ions' mobility, before each experiment the vessel was vacuum pumped down to pressures of 10^{-6} to 10^{-7} Torr and a strict gas filling procedure was carried out. No measurement was considered until the signal stabilised, and all measurements were done in a 2–3 minutes time interval to ensure minimal contamination of the gas mixture, mainly due to outgassing processes.

The method described together with the knowledge of the dissociation channels, product distribution and rate constants represent a valid, although elaborate, solution to the ion identification problem.

3 Results and discussion

The mobility of the ions originated in Xe-C_2H_6 mixtures has been measured for different reduced electric fields E/N (from 10 to 25 Td) and 8 Torr pressure at room temperature (293 K).

The range of the reduced electric field values used to determine the ions' mobility is limited by two distinct factors: one is the electric discharges that occur at high E/N and the limit of applicability of the low field regime (below about 30 Td). The other is the deterioration of the time of arrival spectra for very low values of E/N (below 5 Td or 1.2 kV $\cdot$ cm^{-1} $\cdot$ bar^{-1}), which has been attributed to collisions between the ions and impurity molecules.

Previous works on the mobilities and ionization processes of Xe [7] and C_2H_6 [10] in their parent gases have already been performed in our group.

The range of E/N values considered in this work is within the conditions of low reduced field ($E/N < 30$ Td for the working pressures used).

2017 JINST 12 P10011

3.1 Xenon (Xe)

Regarding the pure xenon (Xe) case, only one peak is observed for electron impact energy of about 20 eV using a reduced electric field of 15 Td and a pressure of 8 Torr at room temperature. The ion responsible for the peak observed is the Xe dimer ion (Xe_2^+). While the atomic ion (Xe^+) is a direct result of electron impact ionization (see [24]), Xe_2^+ is the result of the following reaction:

$$Xe^+ + 2Xe \rightarrow Xe_2^+ + Xe \tag{3.1}$$

Table 1: Ionization products, ionization cross sections for electron impact (20 eV) on Xe [24], appearance energy (A.E) [25] and respective reaction rates.

Reaction	Cross Sec. (10^{-16}cm^2)	A. E. (eV)	Rate Const.	Ref.
$e^- + Xe \rightarrow Xe^+ + 2e^-$	2.43	12.13	-	[24, 25]
$Xe^+ + Xe \rightarrow Xe + Xe^+$	-	-	2.5×10^{-10} cm$^3 \cdot$ s^{-1}	[26]
$Xe^+ + 2Xe \rightarrow Xe_2^+ + Xe$	-	-	2.0×10^{-31} cm$^6 \cdot$ s^{-1}	[27]

3.2 Ethane (C_2H_6)

In pure C_2H_6 two peaks have been observed as reported in a previous work [10]. These two peaks were identified as corresponding to two groups of ions: 3-carbon ($C_3H_n^+$) and 4-carbon ($C_4H_n^+$) ions, which result from reactions involving intermediary products and C_2H_6 molecules. Following direct electron impact ionization the primary ions (CH_3^+, $C_2H_2^+$, $C_2H_3^+$, $C_2H_4^+$, $C_2H_5^+$ and $C_2H_6^+$) are formed (table 2), but they rapidly undergo reactions, which transform them into secondary ions, these being the end products collected at the grid.

Table 3 presents a summary of the possible reactions along with their product distribution and respective reaction rates, for the processes between the ions resulting from primary ionization (table 2), and C_2H_6 molecules, at room temperature.

Table 2: Ionization products, ionization cross sections for electron impact (20 eV) on C_2H_6 [28], appearance energies (A.E) [29] and respective product distribution.

Reaction	Cross Sec. (10^{-16}cm^2)	A. E. (eV)	Prod. Dist.	Ref.
$e^- + C_2H_6 \rightarrow C_2H_6^+ + 2e^-$	0.168	11.57	0.15	[28, 29]
$e^- + C_2H_6 \rightarrow C_2H_5^+ + H^- + e^-$	0.122	12.08	0.11	[28, 29]
$e^- + C_2H_6 \rightarrow C_2H_4^+ + H_2 + 2e^-$	0.490	11.81	0.44	[28, 29]
$e^- + C_2H_6 \rightarrow C_2H_3^+ + H^- + H_2 + e^-$	0.135	14.50	0.12	[28, 29]
$e^- + C_2H_6 \rightarrow C_2H_2^+ + 2H_2 + 2e^-$	0.080	14.41	0.07	[28, 29]
$e^- + C_2H_6 \rightarrow CH_3^+ + CH_3 + 2e^-$	0.032	13.72	0.03	[28, 29]

From tables 2 and 3 two groups of ions become evident as already mentioned: one with 3-carbons — $C_3H_n^+$ (n = 5,6,7,8 and 9) and another with 4-carbons — $C_4H_n^+$ (n = 5,7 and 9) [10]. Nevertheless, their relative abundance is not fully explained by the data in the tables 2 and 3. In fact,

2017 JINST 12 P10011

the unexpected higher relative abundance of $C_4H_n^+$ can be explained by the fact that the primary ion — $C_2H_4^+$ may not lead to $C_3H_7^+$ as shown in table 3, but to an intermediary product, $C_4H_{10}^+$ due to the incomplete reaction between $C_2H_4^+$ and C_2H_6 at 293 K (our experimental conditions). This is, according to [30], a 2-step reaction:

$$C_2H_4^+ + C_2H_6 \rightarrow C_4H_{10}^+ \tag{3.2}$$

$$C_4H_{10}^+ \rightarrow C_3H_7^+ + CH_3 \tag{3.3}$$

Table 3: Possible reactions, product distribution and rate constants for the collisions of the primary ions with C_2H_6. Adapted from [31].

Reaction	Rate Const. (10^{-9} cm$^3 \cdot$ s^{-1})	Prod. Dist.	Ref.
$C_2H_6^+ + C_2H_6 \rightarrow C_3H_8^+ + CH_4$	$0.019^{+}_{-}0.001$	0.42	[32, 33]
$C_2H_6^+ + C_2H_6 \rightarrow C_3H_9^+ + CH_3$	$0.019^{+}_{-}0.001$	0.58	[32, 33]
$C_2H_5^+ + C_2H_6 \rightarrow C_4H_9^+ + H_2$	$0.040^{+}_{-}0.003$	1.00	[33]
$C_2H_4^+ + C_2H_6 \rightarrow C_3H_6^+ + CH_4$	$0.0053^{+}_{-}0.0001$	0.07	[32, 33]
$C_2H_4^+ + C_2H_6 \rightarrow C_3H_7^+ + CH_3$	$0.0053^{+}_{-}0.0001$	0.93	[32, 33]
$C_2H_3^+ + C_2H_6 \rightarrow C_2H_5^+ + C_2H_4$	$0.62^{+}_{-}0.03$	0.47	[33]
$C_2H_3^+ + C_2H_6 \rightarrow C_3H_5^+ + CH_4$	$0.62^{+}_{-}0.03$	0.40	[33]
$C_2H_3^+ + C_2H_6 \rightarrow C_4H_7^+ + H_2$	$0.62^{+}_{-}0.03$	0.13	[33]
$C_2H_2^+ + C_2H_6 \rightarrow C_2H_4^+ + C_2H_4$	$1.46^{+}_{-}0.06$	0.18	[32, 33]
$C_2H_2^+ + C_2H_6 \rightarrow C_2H_5^+ + C_2H_3$	$1.46^{+}_{-}0.06$	0.09	[32, 33]
$C_2H_2^+ + C_2H_6 \rightarrow C_3H_3^+ + CH_3 + H_2$	$1.46^{+}_{-}0.06$	0.06	[32, 33]
$C_2H_2^+ + C_2H_6 \rightarrow C_3H_5^+ + CH_3$	$1.46^{+}_{-}0.06$	0.54	[32, 33]
$C_2H_2^+ + C_2H_6 \rightarrow C_4H_5^+ + H_2 + H$	$1.46^{+}_{-}0.06$	0.05	[32, 33]
$C_2H_2^+ + C_2H_6 \rightarrow C_4H_7^+ + H$	$1.46^{+}_{-}0.06$	0.09	[32, 33]
$CH_3^+ + C_2H_6 \rightarrow C_2H_5^+ + CH_4$	$1.74^{+}_{-}0.06$	0.85	[33]
$CH_3^+ + C_2H_6 \rightarrow C_3H_5^+ + 2H_2$	$1.74^{+}_{-}0.06$	0.09	[33]
$CH_3^+ + C_2H_6 \rightarrow C_3H_7^+ + H_2$	$1.74^{+}_{-}0.06$	0.06	[33]

3.3 Xe-C_2H_6 mixture

In xenon-ethane (Xe-C_2H_6) mixtures, starting with pure C_2H_6 (0% Xe) and up to pure Xe (100% Xe) two peaks were continuously observed. The ions responsible for these peaks are the two groups identified in pure C_2H_6: $C_3H_n^+$ (with higher mobility) and $C_4H_n^+$ (the most intense). Since the electron impact ionization cross section of Xe [24] is higher than that of C_2H_6 [28], it is expected that even for low concentrations of Xe (down to about 30% of Xe), Xe^+ ions are preferentially produced. These Xe^+ ions rapidly undergo one of the possible reactions with C_2H_6, as shown by the rate constants in table 4, rather than with Xe (reaction (3.1)).

The reactions involving Xe^+ ions and C_2H_6 molecules lead to the formation of some of the primary ions found in pure C_2H_6 ($C_2H_4^+$, $C_2H_5^+$ and $C_2H_6^+$), which will also react with the C_2H_6 molecules (see table 3) producing mainly ions with 3-carbons ($C_3H_7^+$, $C_3H_8^+$ and $C_3H_9^+$) but also

2017 JINST 12 P10011

Table 4: Reactions involving Xe atomic ions and its ionization products with C_2H_6. The uncertainty on the reactions presented was 20% according to the information given in [34]. The present table was adapted from [34, 35].

Reaction	Rate Const. (10^{-10} cm$^3 \cdot$ s^{-1})	Prod. Dist.	Ref.
$Xe^+ + C_2H_6 \rightarrow C_2H_6^+ + Xe$	9.20±1.84	0.35	[35]
$Xe^+ + C_2H_6 \rightarrow C_2H_5^+ + H + Xe$	9.20±1.84	0.08	[35]
$Xe^+ + C_2H_6 \rightarrow C_2H_4^+ + H_2 + Xe$	9.20±1.84	0.55	[35]
$Xe_2^+ + C_2H_6 \rightarrow XeC_2H_6^+ + Xe$	6.80±1.36	1.00	[35]

ions with 4-carbons ($C_4H_9^+$ and $C_4H_{10}^+$). However, there is a slight difference between the pure C_2H_6 and the Xe-C_2H_6 case — the supression of $C_2H_3^+$, $C_2H_2^+$ and CH_3^+. As observed in pure C_2H_6, the reaction involving $C_2H_4^+$ with C_2H_6 is incomplete, therefore contributing to the $C_4H_n^+$ peak area instead of to $C_3H_n^+$.

In figure 1 several time of arrival spectra are presented, where 2 peaks are clearly observed, the main and slower corresponding to the 4-carbon group and the faster and smaller to the 3-carbon group, as in pure ethane. Increasing the Xe concentration in the mixture both the peaks' area and ion mobility decrease.

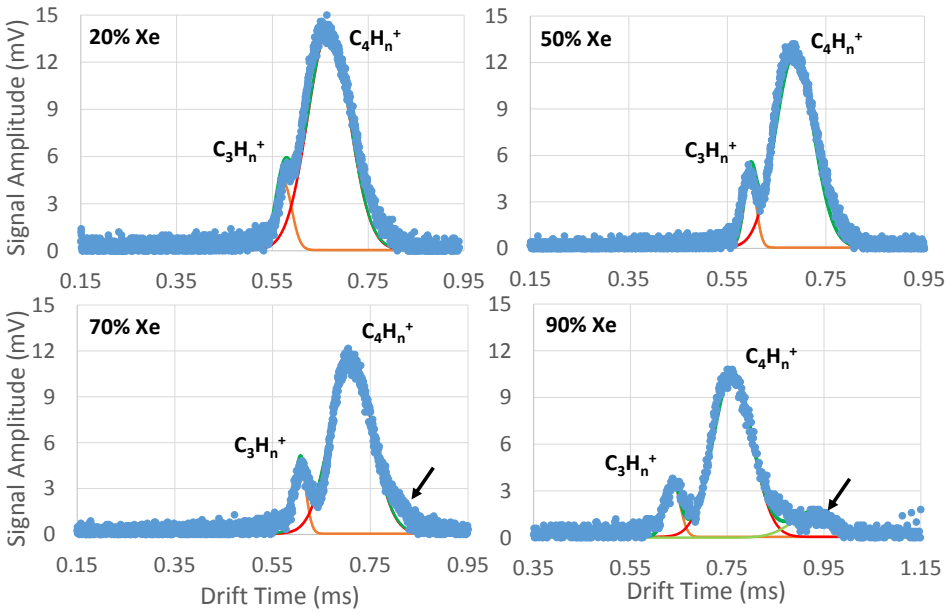

Figure 1: Time-of-arrival spectra of an average of 128 pulses recorded for several Xe-C_2H_6 mixtures (20%, 50%, 70% and 90% of Xe) at a pressure of 8 torr, temperature of 293 K and for a reduced electric field of 20 Td with a voltage across GEM of 20 V (background noise was subtracted). The ions responsible for the peaks appearing in this time-of-arrival spectra are $C_3H_n^+$ (n = 5,6,8,9) and $C_4H_n^+$ (n = 7,9,10).

2017 JINST 12 P10011

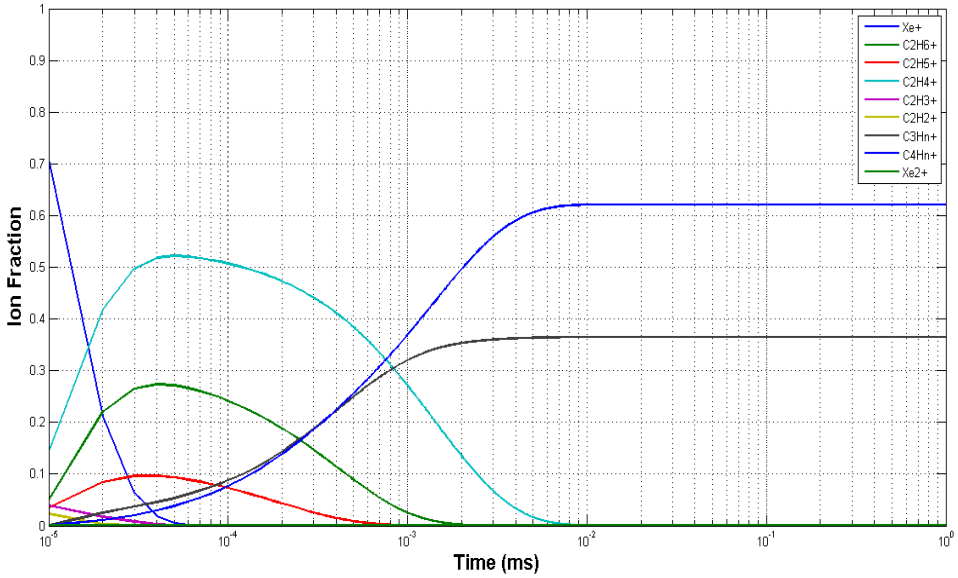

(a)

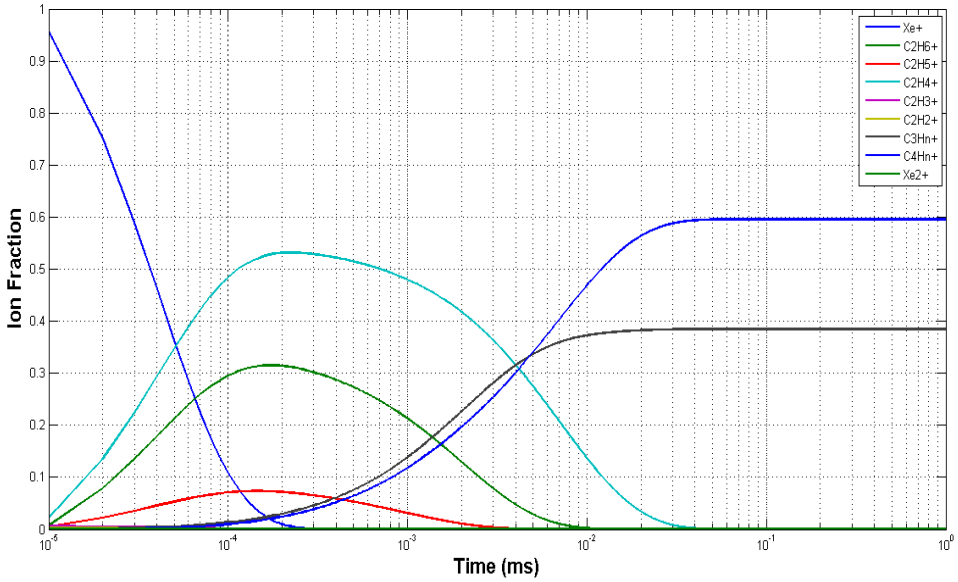

(b)

Figure 2: Fraction of ions that can be formed as a function of time for Xe-C_2H_6 mixtures of 50% (a) and 90% (b) of Xe, for a total pressure of 8 torr.

For Xe concentrations above 70% and for reduced electric fields higher than 20 Td, a small peak starts to appear at the right side of the main one. Looking at table 3 it is possible to see that Xe_2^+ can react with C_2H_6 resulting in $XeC_2H_6^+$ which has a lower mobility than the other ions and could explain the appearance of this bump, meaning that Xe_2^+ would need to be originated under these circumstances. However, since the reaction for the formation of Xe_2^+ (eq. (3.1)) is much slower than the competitive ones displayed in table 3, $XeC_2H_6^+$ is not expected to be present as can be observed in figure 2. In this figure the ion fraction as a function of time, obtained from the cross sections

2017 JINST 12 P10011

and reaction rates for the different primary ions for two Xe concentrations (in figure 2a 50% and in figure 2b 90% of Xe) is presented. As no alternative reaction was found in literature that justifies the presence of this peak, we believe that the mechanism responsible for its appearance is the resonant charge transfer of $C_2H_6^+$ to C_2H_6 [18], which will affect the mobility of the product ions ($C_3H_8^+$ and $C_3H_9^+$), slowing them down. As can be seen, increasing Xe concentration will lead to a significant increase in the reaction time of $C_2H_6^+$ with C_2H_6, which will contribute to the higher influence of the resonant charge transfer on the overall drift time of $C_3H_8^+$ and $C_3H_9^+$, as observed in previous studies [7–9].

In addition, a shift of the peaks towards lower drift times (increasing mobilities) with decreasing Xe concentration can be observed. This effect can be explained by the lower polarizability of Xe atoms and higher reduced mass involved in the collisions of the drifting ions formed with Xe atoms which reduces their mobility, as expressed by the Langevin limit formula (eq. (1.3)).

In order to clarify the ion identification hypothesis given earlier, Blanc's law was used as a cross check method.

Figure 3 shows the reduced mobility of the ions produced in the Xe-C_2H_6 mixture for different mixture ratios for a pressure range of 6–10 Torr and for E/N of 15 Td at room temperature, together with Blanc's law prediction for the main candidate ions — $C_3H_n^+$ (red) and for $C_4H_n^+$ (orange). K_{g1} and K_{g2} in Blanc's law (eq. (1.4)), were obtained either using experimental values from literature or, when not possible, by using the Langevin limit formula (eq. (1.3)).

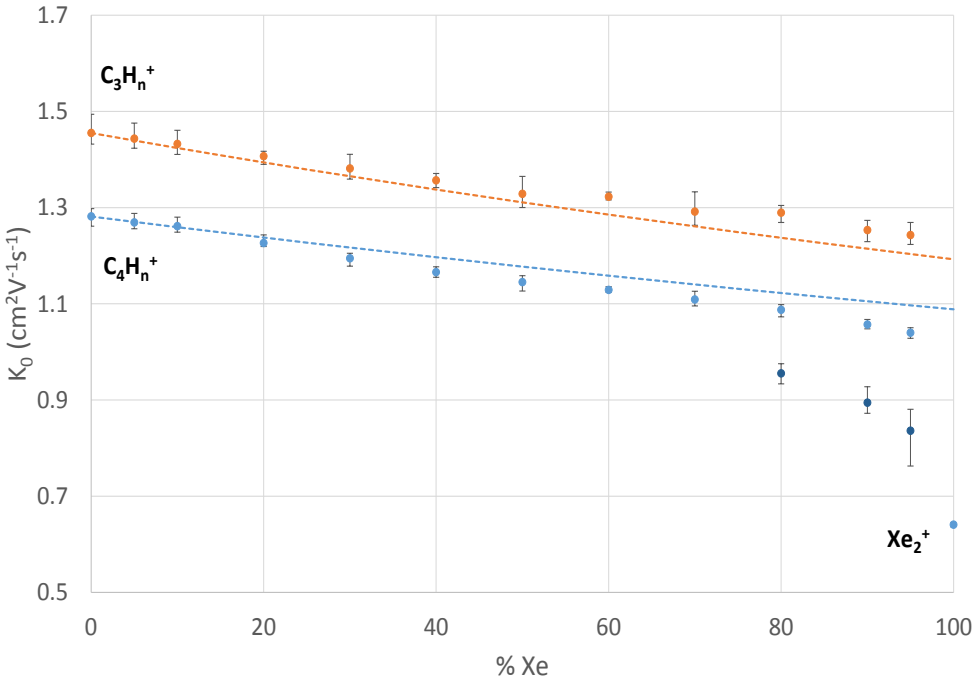

Figure 3: Reduced mobility of the ions produced in the Xe-C_2H_6 mixture for a pressure of 8 Torr and for a E/N of 20 Td at room temperature. The dashed lines represent the mobility values expected from Blanc's law for $C_3H_n^+$ (orange) and for $C_4H_n^+$ (red).

2017 JINST 12 P10011

$C_3H_n^+$ and $C_4H_n^+$ display a small decrease in mobility as Xe percentage increases, both described almost correctly by Blanc's law for all the mixtures studied, except for Xe concentrations above 70%, where a slight deviation from the theoretical curves can be observed. As for the third peak appearing for Xe concentrations above 70%, the mobility was seen to decrease faster than the other peaks, and since a resonant charge transfer is involved in the ion formation process, not much can be expected regarding Blanc's law compliance, as it fails to describe properly such cases. Table 5 summarizes the results obtained.

No significant variation of the mobility was observed in the range of pressures (6-8 Torr) and of E/N (10–25 Td) studied.

Table 5: Mobility of the peaks observed for the Xe-C_2H_6 mixture ratios studied, obtained for E/N of 20 Td, a pressure of 8 Torr at room temperature (298 K).

Mixture	Mobility ($cm^2 \cdot V^{-1} \cdot s^{-1}$)	Ion
Pure C_2H_6	1.28 ± 0.02	$C_4H_n^+$
	1.46 ± 0.03	$C_3H_n^+$
5% Xe	1.27 ± 0.02	$C_4H_n^+$
	1.44 ± 0.03	$C_3H_n^+$
10% Xe	1.26 ± 0.02	$C_4H_n^+$
	1.43 ± 0.03	$C_3H_n^+$
20% Xe	1.23 ± 0.02	$C_4H_n^+$
	1.41 ± 0.03	$C_3H_n^+$
30% Xe	1.19 ± 0.02	$C_4H_n^+$
	1.38 ± 0.03	$C_3H_n^+$
40% Xe	1.17 ± 0.02	$C_4H_n^+$
	1.36 ± 0.02	$C_3H_n^+$
50% Xe	1.14 ± 0.02	$C_4H_n^+$
	1.33 ± 0.03	$C_3H_n^+$
60% Xe	1.13 ± 0.02	$C_4H_n^+$
	1.32 ± 0.03	$C_3H_n^+$
70% Xe	1.11 ± 0.02	$C_4H_n^+$
	1.29 ± 0.03	$C_3H_n^+$
80% Xe	0.96 ± 0.02	-
	1.09 ± 0.02	$C_4H_n^+$
	1.29 ± 0.02	$C_3H_n^+$
90% Xe	0.89 ± 0.02	-
	1.06 ± 0.02	$C_4H_n^+$
	1.25 ± 0.02	$C_3H_n^+$
95% Xe	0.84 ± 0.02	-
	1.04 ± 0.02	$C_4H_n^+$
	1.24 ± 0.02	$C_3H_n^+$
Pure Xe	0.64 ± 0.02	Xe_2^+

4 Conclusion

In the present work we measured the reduced mobility of ions originated by electron impact in the Xe-C_2H_6 mixture under different pressures (from 6 to 10 Torr), low reduced electric fields (from 10 to 25 Td) and different mixture ratios.

Our experimental results seem to be relatively consistent with the ones predicted by the Blanc law throughout the mixture range studied.

The two peaks observed consistently for different concentrations of Xe in the mixture are thought to be originated by 3-carbon ($C_3H_5^+$, $C_3H_6^+$ $C_3H_8^+$ and $C_3H_9^+$) and 4-carbon ($C_4H_7^+$, $C_4H_9^+$ and $C_4H_{10}^+$) ion groups. The ions' mobility were seen to vary with the mixture composition deviating slightly from the theoretical values predicted by Blanc's law for both $C_3H_n^+$ and $C_4H_n^+$, for Xe concentrations above 70%. The $C_4H_n^+$ peak area indicates a higher abundance of this group of ions when compared with the 3-carbon group. For Xe concentrations above 70%, a bump starts to appear at the right side of the main peak for reduced electric fields higher than 20 Td, which was attributed to the resonant charge transfer of $C_2H_6^+$ to C_2H_6 that can affect the mobility of its ion products ($C_3H_8^+$ and $C_3H_9^+$).

Additionally we verified that the experimental mobility values did not display a significant dependence over the studied range of pressure and E/N (6–10 Torr and 10–25 Td, respectively). Future work is expected with other gaseous mixtures. It is our intention to proceed this line of investigation using mixtures such as Ar-N_2 for the ALICE collaboration, Ar-CF_4 and Ar-CF_4-IsoButane (T2K mixture) necessary for the LCTPC collaboration, namely in the ILC/ILD experiment.

Acknowledgments

This work was supported by the RD51 Collaboration/CERN, through the common project "Measurement and calculation of ion mobility of some gas mixtures of interest". André F.V. Cortez received a PhD scholarship from FCT-Fundação para a Ciência e Tecnologia (SFRH/BD/52333/2013).

References

[1] W. Blum and L. Rolandi, *Particle Detection with Drift Chambers*, Springer-Verlag, Berlin Germany (1994).

[2] G.F. Knoll, *Radiation detection and measurements*, John Wiley and Sons Inc., New York U.S.A. (2000).

[3] F. Sauli, *Gaseous Radiation Detectors: Fundamentals and Applications*, *Cambridge Monographs on Particle Physics, Nuclear Physics and Cosmology*, Cambridge University Press, Cambridge U.K. (2014).

[4] G.A. Eiceman, Z. Karpas, and H.H.J. Hill, *Ion Mobility Spectrometry*, third edition, CRC Press – Taylor & Francis Group, Boca Raton U.S.A. (2014).

[5] B. Dolgoshein, *Transition radiation detectors*, *Nucl. Instrum. Meth.* **A 326** (1993) 434.

[6] A. Andronic and J.P. Wessels, *Transition radiation detectors*, *Nucl. Instrum. Meth.* **A 666** (2012) 130.

[7] P.N.B. Neves, C.A.N. Conde and L.M.N. Távora, *Experimental measurement of the mobilities of atomic and dimer Ar, Kr and Xe ions in their parent gases*, *J. Chem. Phys.* **133** (2010) 124316.

2017 JINST 12 P10011

[8] P.N.B. Neves et al., *Experimental measurement of the Ne^+ and Ne_2^+ mobilities in Ne and the reaction rate coefficient for $Ne^+ + 2Ne \rightarrow Ne_2^+ + Ne$*, *IEEE Trans. Nucl. Sci.* **58** (2011) 2060.

[9] A.N.C. Garcia, P.N.B. Neves, A.M.F. Trindade, F.P. Santos and C.A.N. Conde, *A new contribution to the experimental measurement of the N_4^+ and $N_2{}^+$ ion mobility in N2 at 298K*, 2012 *JINST* **7** P02012.

[10] A.F.V. Cortez et al., *Experimental measurement of the mobility of ions originated in ethane in their parent gas*, 2013 *JINST* **8** P07013.

[11] A.F.V. Cortez et al., *Experimental measurements of the mobility of methane ions in Ar-C_2H_6*, 2013 *JINST* **8** P12012.

[12] A.N.C. Garcia et al., *Experimental measurements of the mobility of Xenon- Neon ions mixtures*, 2014 *JINST* **9** P07008.

[13] A.M.F. Trindade et al., *Experimental study on ion mobility in Ar-CH_4 mixtures*, 2014 *JINST* **9** P06003.

[14] P.M.C.C. Encarnação et al., *Experimental Ion Mobility measurements in Ar-CO_2 mixtures*, 2015 *JINST* **10** P01010.

[15] Y. Kalkan, M. Arslandok, A.F.V. Cortez, Y. Kaya, I. Tapan and R. Veenhof, *Cluster ions in gas-based detectors*, 2015 *JINST* **10** P07004.

[16] P.M.C.C. Encarnação et al., *Experimental Ion Mobility measurements in Ne-CO_2 and CO_2-N_2 mixtures*, 2016 *JINST* **11** P05005.

[17] A.F.V. Cortez et al., *Experimental Ion Mobility measurements in Ne-N_2*, 2016 *JINST* **11** P11019.

[18] E.W. McDaniel, J.B.A. Mitchell and M.E. Rudd, *Atomic collisions – heavy particle projectiles*, Wiley, New York U.S.A. (1993).

[19] National Institute of Standards and Technology, Gaithersburg, Maryland, 20899-8320, web address: http://physics.nist.gov/cuu/Constants/Table/allascii.txt.

[20] P. Langevin, *Une formule fondamentale de théorie cinetique*, *Annal. Chim. Phys.* **5** (1905) 245.

[21] R.R. Teachout and R.T. Pack, *The static dipole polarizabilities of all the neutral atoms in their ground states*, *Atom. Data Nucl. Data Tables* **3** (1971) 195.

[22] J.O. Hirschfelder, C.F. Curtis and R.B. Bird, *Molecular Theory of Gases and Liquids*, John Wiley and Sons Inc., New York U.S.A. (1954), pg. 950.

[23] A. Blanc, *Recherches sur le mobilités des ions dans les gaz*, *J. Phys. Theor. Appl.* **7** (1908) 825.

[24] R. Rejoub, B.G. Lindsay, and R.F. Stebblings, *Determination of the absolute partial and total cross sections for electron-impact ionization of the rare gases*, *Phys. Rev.* **A 65** (2002) 042713.

[25] B. Gstir et al., *Electron impact multiple ionization of neon, argon and xenon atoms close to threshold:appearance energies and Wannier exponents*, *J. Phys.* **B 35** (2002) 2993.

[26] H. von Köding, F.A. Pinkse and N.M.M. Nibbering, *Rate Coefficients of Single and Double Electron Transfer from Xe to Xe^{2+} at Low Collision Energies as Determined by Use of Fourier Transform Ion Cyclotron Resonance Mass Spectrometry*, *Physica Scripta* **T 59** (1995) 418.

[27] A.P. Vitols and H.J. Oskam, *Reaction rate constant for $Xe^+ + 2Xe \rightarrow Xe_2^+ + Xe$*, *Phys. Rev.* **A 8** (1973) 1860.

[28] C. Tian and C.R. Vidal, *Electron impact dissociative ionization of ethane: Cross sections, appearance potentials, and dissociation pathways*, *J. Chem. Phys.* **109(5)** (1998) 1704.

[29] E. Vašeková et al., *Electron impact ionization of C_2H_6: ionization energies and temperature effects*, *Int. J. Mass Spectrom.* **235** (2004) 155.

2017 JINST 12 P10011

[30] K. Hiraoka and P. Kebarle, *Ion molecule reactions in ethane. Thermochemistry and structures of the intermediate complexes: $C_4H_{11}^+$ and $C_4H_{10}^+$ formed in the reactions of $C_2H_5^+$* and $C_2H_4^+$ with C_2H_6, *Can. J. Chem.* **58**, (1980) 2262.

[31] W.T. Huntress Jr., *Laboratory studies of bimolecular reactions of positive ions in interstellar clouds, in comets, and in planetary atmospheres of reducing composition*, *Astrophys. J. Suppl.* **33** (1977) 495.

[32] A.S. Blair, E.J. Heslin and A.G. Harrison, *Biomolecular reactions of trapped ions. IV. Reactions in gaseous ethane and mixtures with acetylene and methane-d4*, *J. Am. Chem. Soc.* **94** (1972) 2935.

[33] J.K. Kim, V.G. Anicich and W.T. Huntress Jr., *Product distributions and rate constants for the reactions of CH_3^+, CH_4^+, $C_2H_2^+$, $C_2H_3^+$, $C_2H_4^+$, $C_2H_5^+$, and $C_2H_6^+$ ions with CH_4, C_2H_2, C_2H_4, and C_2H_6*, *J. Phys. Chem.* **81** (1977) 1798.

[34] V.G. Anicich, *Evaluated Bimolecular Gas Phase Kinetics of Psitive Ions for Use in Modeling Planetary Atmospheres, Cometary Comae, and Insterstellar Clouds*, *J. Phys. Chem.* **22** (1993) 6.

[35] K. Giles, N.G. Adams and D. Smith, *Reactions of Kr^+, Kr_2^+, Xe^+ and Xe_2^+ ions with several molecular gases at 300 K*, *J. Phys.* **B 22** (1989) 873.

2017 JINST 12 P10011